Title: Effect of carbon black functionalization on the analytical performance of a tyrosinase biosensor based on glassy carbon electrode modified with dihexadecylphosphate film

Authors: Gisela Ibáñez-Redín, Tiago Almeida Silva, Fernando Campanhã Vicentini, Orlando Fatibello-Filho

PII: S0141-0229(18)30259-X
DOI: https://doi.org/10.1016/j.enzmictec.2018.05.007
Reference: EMT 9215

To appear in: *Enzyme and Microbial Technology*

Received date: 12-1-2018
Revised date: 7-5-2018
Accepted date: 10-5-2018

Please cite this article as: Ibáñez-Redín Gisela, Silva Tiago Almeida, Vicentini Fernando Campanhã, Fatibello-Filho Orlando.Effect of carbon black functionalization on the analytical performance of a tyrosinase biosensor based on glassy carbon electrode modified with dihexadecylphosphate film.*Enzyme and Microbial Technology* https://doi.org/10.1016/j.enzmictec.2018.05.007

Effect of carbon black functionalization on the analytical performance of a tyrosinase biosensor based on glassy carbon electrode modified with dihexadecylphosphate film

Gisela Ibáñez-Redín[1, 2], Tiago Almeida Silva[1], Fernando Campanhã Vicentini[3, *] and Orlando Fatibello-Filho[1]

[1]Department of Chemistry, Federal University of São Carlos, 13560-970 São Carlos, SP, Brazil.

[2]São Carlos Institute of Physics, University of São Paulo, 13566-390 São Carlos, SP, Brazil.

[3]Center of Natural Sciences, Federal University of São Carlos, 18290-000 Buri, SP, Brazil.

*Corresponding author.

Tel.: +55 15 3256 9070

E-mail address: fcvicentini@ufscar.br (Prof. Dr. Fernando C. Vicentini)

Graphical abstract

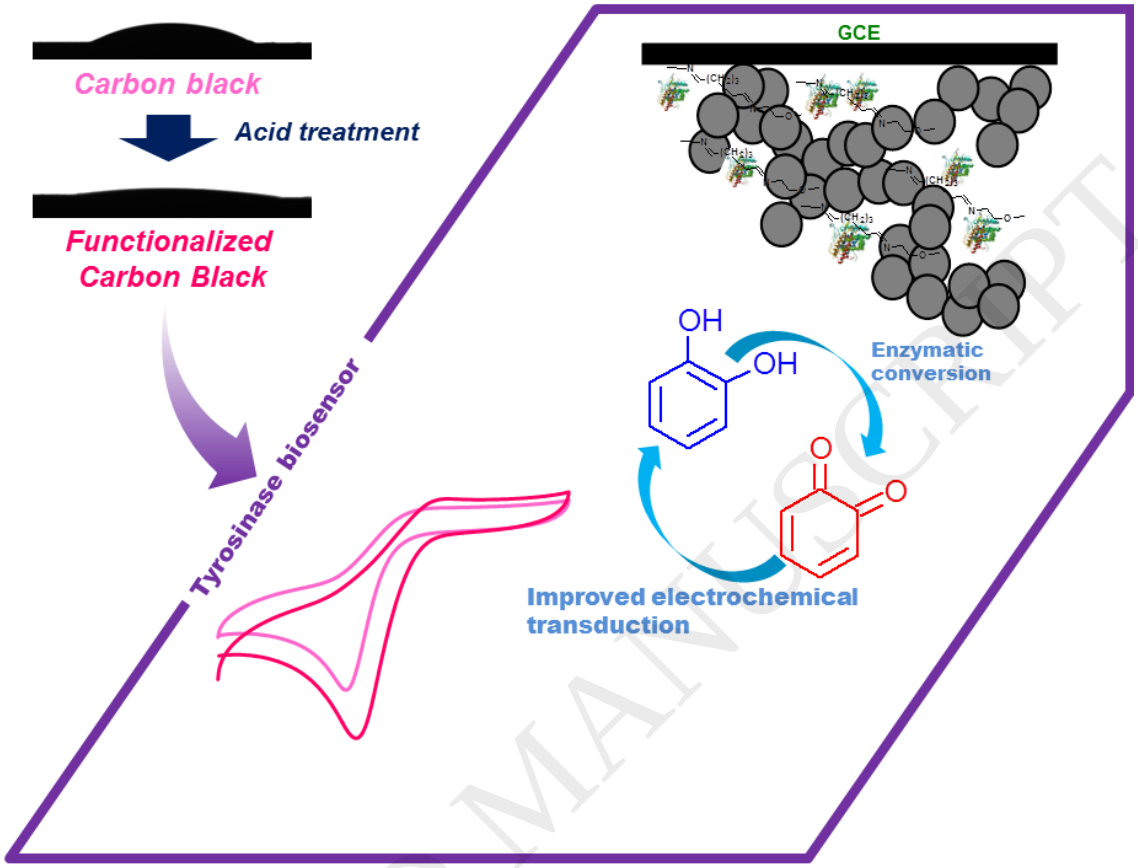

Highlights

- Carbon black (CB) nanoparticles were functionalized by a simple acid treatment
- Functionalized CB (CB-f) provided an improved response for modified electrodes
- CB-f were explored in the design of a tyrosinase (Tyr) biosensor
- Tyr-CB-f based biosensor showed enhanced response toward catechol biosensing

Abstract

Carbon Black (CB) has acquired a prominent position as a carbon nanomaterial for the development of electrochemical sensors and biosensors due to its low price and extraordinary electrochemical and physical properties. These properties are highly dependent on the surface chemistry and thus, the effect of functionalization has been widely studied for different applications. Meanwhile, the influence of CB functionalization over its properties for electroanalytical applications is still being poorly explored. In this study, we describe the use of chemically functionalized CB Vulcan XC 72R for the development of sensitive electrochemical biosensors. The chemical pre-treatment increased the material wettability by raising the concentration of surface oxygenated functional groups verified from elemental analysis and FTIR measurements. In addition, it was observed an enhancement of almost 100-fold on the electron transfer rate constant (k^0) related to unfunctionalized CB, confirming a remarkable improvement of the electrocatalytic properties. Finally, we constructed a Tyrosinase (Tyr) biosensor based on functionalized CB and dihexadecylphosphate (DHP) for the determination of catechol in water samples. The resulting device displayed an excellent stability with a limit of detection of 8.7×10^{-8} mol L^{-1} and a sensitivity of 539 mA mol^{-1} L. Our results demonstrate that functionalized CB provides an excellent platform for biosensors development.

Keywords: carbon black, catechol, chemical functionalization, environmental analysis, enzymatic biosensors.

1. Introduction

Carbon black (CB) is the term used to define a group of carbon materials produced from the combustion or thermal decomposition of different oil products [1]. It has been widely used for different applications ranging from polymers reinforcement [2] to catalysis [3]. Recently, CB has become focus of intensive research for the development of electrochemical sensors and biosensors due to its low cost and, mainly, due to its attractive properties, *e.g.*, high specific surface area, electric conductivity and chemical stability. The use of several kinds of CBs for electroanalytical applications has been successfully explored and it is well documented in the recent literature [4-12].

CBs are mainly composed of carbon and hydrogen; however, there are other elements in their composition such as sulfur, nitrogen and predominantly oxygen [2]. The latter element has the greatest influence on the physicochemical properties of CB: it is chemisorbed on the surface during the production and storage processes and also may be introduced from different functionalization treatments [13]. The effect of CB functionalization has been studied for different applications such as the synthesis of supported metal catalysts [14] and the adsorption of pollutants [15]. Regarding to the applications in electroanalysis, a few works have reported the advantages of using functionalized CB. In this context, Frysz and Chung [16] studied the effect of different pretreatments on the electrochemical properties of CB paste electrodes finding improvements in the performance of the electrodes as result of the increase of oxygenated complex at the material surface. More recently, Arduini *et al*. [5] compared the influence of different functionalization treatments over the properties of CB N220. Their results showed an improvement of the material electrocatalytic properties towards several molecules promoted by the oxidative treatment in acid medium.

CB is an attractive candidate for enzyme immobilization due to its high surface area and large pore volume which are important requirements for enzymes adsorption [17]. This material has a broad pore size distribution ranging from micropore to macropore and has been successfully used as a matrix for enzyme immobilization for analytical purposes [18-20]. Besides the effect over the electrocatalytic properties, the functionalization of porous supports can also lead to enhanced biomolecules immobilization by improving the interactions between the molecules and the material's porous walls [21]. For instance, it has been demonstrated that the adsorption capability to proteins of mesoporous carbon can be enhanced by introducing carboxylic groups at the material surface [22]. The presence of oxygenated functional groups at the support has also being found to influence positively the biomolecules electrocatalytic properties. Matsui *et al.* compared the electrochemical activity of cytochrome c adsorbed on oxidized CB and as received CB, their results have shown that oxidized material is more effective to promote and maintain the cytochrome c activity [23]. Nevertheless, despite the great attention attracted by CB in the last years, the development of electrochemical biosensors with functionalized CB is still a much less explored area.

In this paper, we explore the use of functionalized CB as material for the development of electrochemical biosensors. We constructed a tyrosinase (Tyr) biosensor based on functionalized CB and dihexadecylphosphate (DHP), a surfactant molecule with two hydrophobic long chains and a negatively charged phosphate group that have been extensively used for the preparation of stable films in the development of electrochemical sensors [24,25] and biosensors [26]. The influence of CB functionalization on some of its properties was evaluated through scanning electron microscopy (SEM), Fourier transform infrared spectroscopy (FTIR), elemental analysis and contact angle measurements. Using a crosslinking technique, Tyr was immobilized onto the surface of a glassy carbon electrode (GCE) modified with functionalized CB and DHP. Operating

and analytical parameters of the biosensor towards the amperometric detection of catechol were evaluated as well as the apparent kinetic behaviour of the immobilized enzyme.

2. Experimental

2.1. Reagents, solutions and samples

Tyr from mushroom (≥ 1000 U mg^{-1}), bovine serum albumin (BSA), DHP, potassium hexacyanoferrate (III), and catechol were obtained from Sigma-Aldrich. CB Vulcan XC 72R was received from Cabot Corporation. All chemicals were of analytical grade and the solutions were prepared with Milli-Q ultrapure water with resistivity no less than 18 MΩ cm. 0.1 mol L^{-1} sodium phosphate buffer solutions were prepared using NaH_2PO_4 and Na_3PO_4. Water samples were collected from a lake at Federal University of São Carlos (São Carlos, Brazil). The samples were spiked with a known catechol concentration and directly analyzed using the proposed procedure.

2.2. Apparatus

All the electrochemical measurements were carried out using a three electrode cell with working volume of 10 mL. The Tyr biosensor was used as working electrode and a platinum plate and Ag/AgCl (3 mol L^{-1} KCl) were used as counter and reference electrodes, respectively. The amperometric and cyclic voltammetric (CV) measurements were performed using a μAutolab Type III potentiostat/galvanostat (Ecochemie, Netherlands) controlled with GPES 4.9 software. The electrochemical impedance spectroscopy (EIS) experiments were performed using an Autolab PGSTAT-30 potentiostat/galvanostat (Ecochemie). The frequency range used was 100 mHz to 100 kHz.

For SEM and contact angle measurements, 8 µL of an aqueous dispersion of CB (1 mg mL^{-1}) were deposited onto a glassy carbon plate surface and allowed to dry at 25 °C for 2 h. SEM images were obtained using a Supra 35-VP equipment (Carl Zeiss, Germany) with electron beam energy of 25 keV. Contact angle experiments were performed at a HTM Reetz goniometer GMBH model DSAHT-12 (Kross) controlled by DSA 3 Image software. For the angle measurement, 3 µL of ultrapure water were added onto the substrate. Three angle measurements were made for each sample; the average and standard deviation were also calculated. The surface chemistry of CB was characterized by mean FTIR. FTIR spectra were recorded using KBr pellets in a Perkin Elmer 1600 spectrophotometer. The CB samples were dried during 12 h in oven at 120 °C, and then 1 mg of CB was mixed with 200 mg of dried KBr to record the spectra. The chemical composition of CBs was accessed by elemental analysis (EA). EA was performed using a FlashEA analyzer (Thermo) to obtain the percentages of carbon, hydrogen, nitrogen and sulfur at each sample. The oxygen percentage was calculated by subtraction of the other elements content.

2.3. Functionalization of CB

For the functionalization treatment, 50 mg of CB were mechanically stirred in the presence of 100 mL of concentrated nitric and sulfuric acids 1:1 (v/v) mixture for 30 min at 25 °C. After this, the samples were thoroughly washed with ultrapure water, centrifuged and redispersed. This sequence was repeated until reaching pH 6.5–7.0 for the supernatant washing water and then dried at 120 °C for 12 h. The functionalized CB was denoted as CB-f.

2.4. Preparation of Tyr-CB-f-DHP/GCE biosensor

Prior to modification, a GCE (diameter: 3 mm) was polished with 0.3 and 0.05 μm alumina slurries and washed with ultrapure water. Then, it was sonicated in isopropyl alcohol and ultrapure water for 5 min each time. The CB dispersions were prepared as previously described [8], i.e., by ultrasonication for 30 min of a mixture containing 1.0 mg of CB (or CB-f), 1.0 mg of DHP and 1.0 mL of ultrapure water. For the GCE modification, 8 μL of this dispersion was dropped onto the electrode surface and the solvent was allowed to evaporate during 2 h at room temperature. The modified GCE electrodes were denoted as CB-DHP/GCE and CB-f-DHP/GCE.

For the enzyme immobilization, a mixture of 3 μL of Tyr solution (20 U μL^{-1} in 0.1 mol L^{-1} phosphate buffer solution pH 7.0), 2 μL of 0.1% m/v BSA solution and 2 μL of 0.25% v/v GA solution was coated onto the modified GCE surface and dried at room temperature. The biosensor was labelled as Tyr-CB-f-DHP/GCE. For the electrochemical study, a biosensor using unmodified CB (Tyr-CB-DHP/GCE) was prepared on parallel for comparison purposes.

3. Results and Discussion

3.1. Material characterization

The initial goal of this study was to determinate the effect of CB Vulcan XC 72R functionalization over its physicochemical properties. We first investigated the structural changes promoted by the pretreatment. The CB structure is composed by spherical particles with diameter between 10 and 500 nm, which combine to form aggregates and agglomerates of different sizes and shapes. We used SEM to visualize the material morphology. Fig. 1 shows the SEM images of CB before (a) and after (b) oxidative treatment. Both surfaces exhibited the typical CB morphology with significant roughness and spherical particles. In a previous study, it was reported that some functionalization treatments significantly can alter the CB morphology resulting on a diminution of the material surface area [15]. In this study, significant differences

between the SEM images for CB and CB-f were not observed. In both cases, a good distribution of the material on the surface of GCE substrate was observed suggesting the retention of the surface morphology after the functionalization treatment.

The chemical composition of the CB samples was estimated by elemental analysis as presented in Table S1 (Please, see "Electronic Supplementary Material"). The presence of nitrogen, sulfur and oxygen in addition to carbon and hydrogen was detected. The C:O molar ratio was predicted for CB and CB-f samples, and this parameter decreased from 17.5 in the CB case for 3.2 in the CB-f case. As expected, a decrease in the carbon content and an increase in the oxygen content as a result of functionalization were observed. This behaviour is attributed to the oxidation of the aromatic structure of the material and the introduction of oxygenated functional groups. An increment in the nitrogen content ascribed to the formation of nitro and nitrate aromatic compounds [28] was also detected.

FTIR has been widely used as a tool for the analysis of carbon material structures. We used FTIR to investigate the change at the CB functional groups caused by the functionalization treatment. The FTIR spectra recorded for CB and CB-f are shown in Fig. S1. For both samples, characteristic bands related to the presence of oxygenated functional groups were observed. Both spectra exhibited a band at 1609 cm^{-1} attributed to the C=C stretching vibrations in aromatic structures [29] and a band around 1711 cm^{-1} related to the C=O stretching vibrations of lactone, aldehyde, ketone and carboxylic groups present in the polyaromatic structure of carbon materials [15]. The bands at 1160 cm^{-1} (CB) and 1175 cm^{-1} (CB-f) can be assigned to the stretching vibrations of C-O bonds commonly occurring between 1150 and 1300 cm^{-1} [30]. The band at 1400 cm^{-1} observed for CB has been related to C-OH vibration [31] and the sharped peaks between 2300-2400 in CB-f can be associated to O-H stretching vibrations from strongly hydrogen-bonded -COOH [32]. It is worth noting the presence of a broad band centered at 3405

cm^{-1} associated to O-H stretching vibrations, the intensity of this band is greater on CB-f, which may be attributed to an increase in oxygenated groups due to the functionalization treatment.

The modification of CB surface with the oxidative treatment was also confirmed by contact angle measurements with water. As shown in Fig. S2, the contact angle decreased drastically after the functionalization treatment. The contact angles obtained for CB and CB-f were (40.6 ± 0.4)° and (11.0 ± 0.3)°, respectively, indicating a large increase of the material hydrophilicity and wettability for polar solvents provided by the introduction of oxygenated species at the surface.

3.2. Electrochemical characterization of CB-DHP/GCE and CB-f-DHP/GCE

The electrochemical characterization was done by means of EIS using as redox probe $K_3[Fe(CN)_6]$. In order to produce stable films over the GCE substrate, we used DHP in combination with CB or CB-f for the GCE modification. The impedance spectra were recorded in 0.1 mol L^{-1} KCl solution containing 1.0×10^{-3} mol L^{-1} $K_3Fe(CN)_6$ at the formal potential of the redox pair $[Fe(CN)_6]^{3-/4-}$ (GCE: +0.211 V; CB-DHP/GCE: +0.213 V and CB-f-DHP/GCE: +0.223 V, respectively).

The Nyquist plots for the different electrodes are shown in Fig. 2. In all cases, it was observed a semicircle at high frequencies and a linear region at low frequencies, which represents the kinetic and diffusional processes, respectively. The charge-transfer resistance (R_{ct}) values for the electrodes were calculated from the semicircle diameter of Nyquist plots. The unmodified GCE exhibited a R_{ct} of 21.4 kΩ, which increased significantly with the introduction of DHP at the electrode surface, as can be seen in Fig 2. (Inset (a)). This behaviour has been previously observed for GCE modified with DHP and is attributed to the partial blockage of the electron transfer [33]. Then, the R_{ct} decreased to 9.46 kΩ from the incorporation of CB at the electrode

surface. This find can be associated to the fast electronic transfer through the modified interface and to the increment of the amount of defect sites on the surface [6]. Furthermore, the smallest R_{ct} value (102.6 Ω) was obtained when CB-f was used, as can be observed in Fig. 2. (Inset (b)), indicating an enhancement of the electrode conductivity promoted by the CB functionalization.

To obtain more detailed information about the effect of CB functionalization over its electrochemical properties, the apparent heterogeneous electron transfer rate constant (k^0_{app}) was estimated using the equation:

$$k^0_{app} = \frac{RT}{F^2 A R_{ct} C} \quad (1)$$

where C is the $K_3[Fe(CN_6)]$ concentration (1.0×10^{-6} mol cm^{-3}), A is the electrode geometric area (0.072 cm^2) and R (8.314 J mol^{-1}), T (298.15 K), and F (96 485 C mol^{-1}) have their usual meanings. The k^0_{app} obtained for GCE, CB-DHP/GCE and CB-f-DHP/GCE were 1.7×10^{-4}, 3.9×10^{-4} and 3.6×10^{-2} cm s^{-1}, respectively. Thus, the use of CB-f increased the electron transfer rate towards the redox pair $[Fe(CN_6)]^{3-/4-}$ in almost 100 times relatively to unfunctionalized CB. The electronic transfer enhancement promoted by acidic treatment agrees with results previously obtained for functionalized CB [15] and CNTs [34] and it is attributed to the increase in the number of defects in the material structure, as well as the increase in the concentration of surface oxygenated groups.

3.3 Tyr-CB-f-DHP/GCE biosensor

In order to evaluate the suitability of CB-f for biosensors development, we constructed a Tyr biosensor based on DHP and CB-f. Different immobilization techniques were evaluated (data not shown) and the most stable film was obtained for a cross-linking technique with

glutaraldehyde and BSA. Therefore, this technique was selected for the biosensor construction. Catechol was chosen as a model of phenolic compounds for the analytical assay of the biosensor. The electrochemical behaviour of catechol at the biosensor was studied by means of cyclic voltammetry (CV). Fig. 3 shows the CVs recorded for (a) Tyr-CB-DHP/GCE and (b) Tyr-CB-f-DHP/GCE before and after the addition of 1.0×10^{-4} mol L^{-1} catechol in 0.1 mol L^{-1} phosphate buffer solution (pH 7.0). In the absence of catechol, redox peaks were not observed, indicating the lack of direct electron transfer between the enzyme and the electrode surface. After the addition of catechol, the reduction current increased for both electrodes due to the electrochemical reduction of *o*-quinone produced in the enzymatic reaction of catechol with oxygen catalysed by tyrosinase. As observed, the functionalization of CB leads to an increment in the reduction peak current. The current intensity at Tyr-CB-f-DHP/GCE was approximately 30% higher than that obtained using Tyr-CB-DHP/GCE. This behaviour can be attributed to the improvement of CB electrocatalytic properties promoted by the functionalization treatment in addition to the enhancement on the enzyme catalytic activity promoted by the interaction with carboxylic and hydroxyl groups [23]. These results suggest an advantage of CB functionalization for the development of electrochemical biosensors.

3.4. Optimization of experimental parameters

The influence of pH on the reduction of catechol using the proposed biosensor was evaluated using 0.1 mol L^{-1} phosphate buffer solutions over the range of 5.5 to 8.0. Fig. 4 shows the CVs for a 1.0×10^{-4} mol L^{-1} catechol solution. It can be noted that the activity of the enzyme is strongly dependent on solution pH. An increase of pH caused an increment of cathodic peak current up to pH 7.5. We also investigated the influence of the electrolyte solution concentration on the biosensor response for phosphate buffer solutions over the range from 0.01 to 0.2 mol L^{-1}.

The CVs obtained for a catechol concentration of 1.0×10^{-4} mol L^{-1} in phosphate buffer solutions at pH 7.5 are shown at Fig. S3. The best analytical signal was observed at 0.075 mol L^{-1} phosphate buffer solution. As can be seen in Fig. S3 (inset), the current signal decreased for concentrations higher than 0.075 mol L^{-1}, and this behaviour can be attributed to the competition between the substrate catechol and phosphate groups for the enzyme active site [35]. Considering these results, a 0.075 mol L^{-1} phosphate buffer solution at pH 7.5 was selected as supporting electrolyte for all subsequent experiments.

3.5. Amperometric determination of catechol

Tyr-CB-f-DHP/GCE was used for the amperometric determination of catechol under optimized experimental conditions. Fig. 5 shows the amperometric response of the biosensor for different concentrations of catechol in the range from 1.0×10^{-6} to 3.9×10^{-5} mol L^{-1}. The analytical curve for catechol is also presented at Fig. 5. The biosensor exhibited a saturation behaviour at high substrate concentrations, which is a typical behaviour of a Michaelis-Menten mechanism. The analytical curve was linear for catechol in the concentration range from 1.0 $\times 10^{-6}$ to 1.9 $\times 10^{-5}$ mol L^{-1}. The linear regression equation correspondent to the analytical curve was: ΔI_p (μA) = $-0.21 + 5.4 \times 10^5$ [catechol] (mol L^{-1}) with a correlation coefficient of 0.997. The limit of detection (LOD) calculated as three times the standard deviation of the blank solution divided by the slope of the analytical curve was found to be 8.7×10^{-8} mol L^{-1}. The analytical parameters of Tyr-CB-f-DHP/GCE were compared with those previously reported in the literature using Tyr based biosensors for the determination of catechol (Table 1). The proposed method showed a lower LOD than the biosensors [26, 36-40], a remarkably higher sensitivity than the biosensors [26, 36-41] and a higher LOD and lower sensitivity than the

devices reported on [42, 43]. Additionally, the proposed biosensor is cost optimal due to the use of CB, a less expensive material compared to most of materials used in the reported studies.

The apparent Michaelis-Menten constant (K_M^{app}) for the immobilized enzyme was calculated from Lineweaver-Burk equation:

$$\frac{1}{I_s} = \frac{1}{I_{max}} + \frac{K_M^{app}}{I_{max}} \times \frac{1}{[\text{Catechol}]} \quad (2)$$

where I_s is the steady state current after the addition of catechol and I_{max} is the maximum current of the system obtained at enzyme saturation conditions. The K_M^{app} value for Tyr immobilized at CB-f and DHP was estimated to be 2.0×10^{-5} mol L^{-1}, which indicate a high affinity of the immobilized enzyme to catechol substrate. The K_M^{app} found in this study was much lower than that obtained for free Tyr (4.0×10^{-3} mol L^{-1}) [44], indicating that CB-f-DHP provides an excellent matrix for Tyr immobilization. This behaviour is attributed to the enzyme stabilization by the immobilization inside the mesoporous material, which prevents the protein unfolding [45], in addition to the effective entrapment on the DHP-GA-BSA matrix. The Tyr enzyme immobilized at CB-f also exhibited a lower K_M^{app} value than that reported for the enzyme immobilized on different surfaces as GCE modified with Nafion and zinc oxide nanoparticles (1.7×10^{-3}mol L^{-1}) [36] and platinum modified with polypyrrole (1.0×10^{-1} mol L^{-1}) [46].

3.6. Stability, interference and recovery studies

To assess the biosensor stability, the intra- (n = 5) and inter-day (n = 3) repeatabilities were studied monitoring the current signal for a 5.0×10^{-6} mol L^{-1} catechol in a 0.075 mol L^{-1} phosphate buffer solution (pH 7.5) using the same biosensor. Relative standard deviation values (RSD) of 3.3% and 3.8% were obtained for intra- and inter-day studies, respectively. These

results demonstrated good measurement precision of the proposed method, which is a consequence of the good stability achieved from the immobilization of the Tyr enzyme on the proposed electrode architecture based on functionalized CB. The biosensor fabrication reproducibility was evaluated from the comparison of the catechol response recorded using three electrodes constructed by the same procedure. The RSD for the amperometric response of 5.0×10^{-6} mol L^{-1} catechol was found to be 7.8%, indicating the high biosensor fabrication reproducibility. We emphasize that the achieved excellent fabrication reproducibility was possible due to the simplicity of the procedure adopted for construction of the electrochemical biosensor.

In addition, the potential interference of other substances that could be found in water samples was also investigated. Amperometric response toward the addition of 5.0×10^{-5} mol L^{-1} of Mg^{2+}, CO_3^{2-}, K^+, Cl^-, Cu^{2+}, Fe^{3+}, PO_4^{3-} and naphthol was evaluated in the presence of 5.0×10^{-6} mol L^{-1} catechol in a 0.075 mol L^{-1} phosphate buffer solution (pH 7.5). As it can be seen at the Fig. 6, all tested species at 10 times catechol concentration had a negligible interference effect on catechol detection. All species caused changes at current signal lower than 5.7%, indicating the suitability of the proposed biosensor to determinate catechol in water samples without matrix-significant interference. To demonstrate the potential application of Tyr-CB-f-DHP/GCE biosensor, the recovery test of spiked catechol in water samples was carried out. Table 2 contains the recoveries percentages obtained for different catechol concentrations, and the values ranged from 94% to 99%, indicating that the proposed biosensor is appropriated for the determination of catechol in water samples.

4. Conclusions

In this study, we demonstrated the suitability of functionalized carbon black (CB-f) as material for the development of electrochemical biosensors. The functionalization increased the material oxygen content and significantly enhanced its wettability. The CB electrochemical properties were also remarkably influenced by the functionalization. From impedance studies, the electrode modified with CB-f exhibited an electron transfer for the redox pair $[Fe(CN)_6]^{3-/4-}$ ~100 times faster as compared with the unfunctionalized CB. Tyrosinase biosensor prepared with the CB-f-DHP matrix exhibited a better response towards catechol than the biosensor obtained with unfunctionalized CB-DHP. The Tyr-CB-f-DHP/GCE biosensor was applied to the amperometric detection of catechol with attractive analytical parameters such as good response stability, low limit of detection, high sensitivity and high affinity to catechol. Because of its simple fabrication process, low cost and good electrochemical properties, the proposed architecture has great potential as immobilization matrix for the development of electrochemical biosensors.

Acknowledgments

The authors acknowledge Brazilian agencies FAPESP (Grant number: 2011/13312-5), CNPq and CAPES for their financial support.

References

[1] C. M. Long, M. A. Nascarella, P. A. Valberg, Carbon black vs. black carbon and other airborne materials containing elemental carbon: Physical and chemical distinctions, Environ. Pollut. 181 (2013) 271-286.

[2] Z. Jiang, J. Jin, C. Xiao, X. Li, Effect of surface modification of carbon black (CB) on the morphology and crystallization of poly (ethylene terephthalate)/CB masterbatch, Colloids. Surf. A Physicochem. Eng. Asp. 395 (2012). 105-115.

[3] A. Moraes, M. H. M. T. Assumpção, F. C. Simões, V. S. Antonin, M. R. V. Lanza, P. Hammer, M. C. Santos, Surface and Catalytical effects on Treated Carbon Materials for Hydrogen Peroxide Electrogeneration, Electrocatalysis. 7 (1) (2016) 60-69.

[4] F. Arduini, A. Amine, C. Majorani, F. Di Giorgio, D. De Felicis, F. Cataldo, G. Palleschi, High performance electrochemical sensor based on modified screen-printed electrodes with cost-effective dispersion of nanostructured carbon black**,** Electrochem . Commun. 12 (3) (2010) 346-350.

[5] F. Arduini, F. D. Giorgio, A. Amine, F. Cataldo, D. Moscone, G. Palleschi, Electroanalytical characterization of carbon black nanomaterial paste electrode: development of highly sensitive tyrosinase biosensor for catechol detection, Anal. Lett**.** 43 (10-11) (2010) 1688-1702.

[6] F. Arduini, F. Di Nardo, A. Amine, L. Micheli, G. Palleschi, D. Moscone, Carbon Black-Modified Screen-Printed Electrodes as Electroanalytical Tools, Electroanalysis. 24(4) (2012) 743-751.

[7] T. W. Lo, L. Aldous, R. G. Compton, The use of nano-carbon as an alternative to multi-walled carbon nanotubes in modified electrodes for adsorptive stripping voltammetry, Sens. Actuators, B. 162 (1) (2012) 361-368.

[8] F. C. Vicentini, A. E. Ravanini, L. C. Figueiredo-Filho, J. Iniesta, C. E. Banks. O. Fatibello-Filho, Imparting improvements in electrochemical sensors: evaluation of different carbon blacks that give rise to significant improvement in the performance of electroanalytical sensing platforms, Electrochim. Acta. 157 (2015) 125-133.

[9] D. Talarico, F. Arduini, A. Constantino, M. Del Carlo, D. Compagnone, D. Moscone, G. Palleschi, Carbon black as successful screen-printed electrode modifier for phenolic compound detection. Electrochem. Commun. 60 (2015) 78-82.

[10] P. B. Deroco, F. C. Vicentini, O. Fatibello-Filho, An electrochemical sensor for the simultaneous determination of paracetamol and codeine using a glassy carbon electrode modified with nickel oxide nanoparticles and carbon black, Electroanalysis. 27(9) (2015) 2214-2220.

[11] P. A. Raymundo-Pereira, A. M. Campos, F. C. Vicentini, B. C. Janegitz, C. D. Mendonça, L. N. Furini, N. V. Boas, M. L. Calegaro, C. J. L. Constantino, S. A. S. Machado, O. N. Oliveira-Júnior, Sensitive detection of estriol hormone in creek water using a sensor platform based on carbon black and silver nanoparticles, Talanta 174 (2017) 652-659.

[12] F. Calegari, L.P. De Souza, M. M. Barsan, C.M.A Brett, L. H. Marcolino-Junior, M. F. Bergamini, Construction and evaluation of carbon black and poly(ethyleneco-vinyl)acetate (EVA) composite electrodes for development of electrochemical (bio)sensors, Sens. Actuators. B. 253 (2017) 10–18.

[13] H. P. Boehm, Some aspects of the surface chemistry of carbon blacks and other carbons, Carbon. 32(5) (1994) 759-769.

[14] M. Carmo, M. Linardi, J. G. R. Poco, Characterization of nitric acid functionalized carbon black and its evaluation as electrocatalyst support for direct methanol fuel cell applications, Appl. Catal., A. 355(1) (2009) 132-138.

[15] D. Borah, S. Satokawa, S. Kato, T. Kojima, Characterization of chemically modified carbon black for sorption application, Appl. Surf. Sci. 254(10) (2008) 3049-3056.

[16] C. A. Frysz, D. D. L. Chung, Improving the electrochemical behaviour of carbon black and carbon filaments by oxidation, Carbon. 35(8) (1997) 1111-1127.

[17] Z. Zhou, M. Hartmann, Progress in enzyme immobilization in ordered mesoporous materials and related applications, Chem. Soc. Rev. 42(9) (2013) 3894-3912.

[18] S. Nadifiyine, M. Haddam, J. Mandli, S. Chadel, C. C. Blanchard, J. L. Marty, A. Amine, Amperometric biosensor based on tyrosinase immobilized on to a carbon black paste electrode for phenol determination in olive oil, Anal. Lett. 46(17) (2013) 2705-2726.

[19] M. Portaccio, D. Di Tuoro, F. Arduini, D. Moscone, M. Cammarota, D. G. Mita, M. Lepore, Laccase biosensor based on screen-printed electrode modified with thionine–carbon black nanocomposite, for Bisphenol A detection, Electrochim. Acta. 109 (2013) 340-347.

[20] F. Arduini, M. Forchielli, A. Amine, D. Neagu, I. Cacciotti, F. Nanni, G. Palleschi, Screen-printed biosensor modified with carbon black nanoparticles for the determination of paraoxon based on the inhibition of butyrylcholinesterase, Microchim. Acta. 182 (3-4) (2015) 643-651.

[21] D. N. Tran, K. J. Balkus Jr, Perspective of recent progress in immobilization of enzymes, Acs. Catal. 1 (8) (2011) 956-968.

[22] A. Vinu, K. Z. Hossian, P. Srinivasu, M. Miyahara, S. Anandan, N. Gokulakrishnan, V. V. Balasubramanian, Carboxy-mesoporous carbon and its excellent adsorption capability for proteins, J. Mater. Chem. 17 (18) (2007) 1819-1825.

[23] M. Matsui, J. I. Ozaki, Effect of oxidative treatment of carbon black on electrochemical activity of cytochrome c, Anal. Methods. 4 (6) (2012) 1623-1625.

[24] F. C. Vicentini, A. E. Ravanini, T. A. Silva, B. C. Janegitz, V. Zucolotto, O. Fatibello-Filho, A novel architecture based upon multi-walled carbon nanotubes and ionic liquid to improve the electroanalytical detection of ciprofibrate, Analyst 139 (16) (2014) 3961-3967.

[25] N. B. Simioni, G. G. Oliveira, F. C. Vicentini, M. R. V. Lanza, B. C. Janegitz, O. Fatibello-Filho, Nanodiamonds stabilized in dihexadecyl phosphate film for electrochemical study and quantification of codeine in biological and pharmaceutical samples, Diam. Relat. Mater. 74 (2017), 191-196.

[26] F. C. Vicentini, L. L. C. Garcia, L. C. S. Figueiredo-Filho, B. C. Janegitz, O. Fatibello-Filho, A biosensor based on gold nanoparticles, dihexadecylphosphate, and tyrosinase for the determination of catechol in natural water. Enzyme Microb. Technol. 84 (2016) 17-23.

[27] M. J., Lázaro, L. Calvillo, V. Celorrio, J. I. Pardo, S. Perathoner, R. Moliner, Study and application of carbon black Vulcan XC-72R in polymeric electrolyte fuel cells, in: I. J. Sanders, T. L Peeten (Eds.), Carbon Black: Production, Properties and Uses, Nova Science Publishers, 2011, p. 41.

[28] I. Bautista-Toledo, J. Rivera-Utrilla, M. A. Ferro-Garcia, C. Moreno-Castilla, Influence of the oxygen surface complexes of activated carbons on the adsorption of chromium ions from aqueous solutions: effect of sodium chloride and humic acid, Carbon. 32 (1) (1994) 93-100.

[29] W. Shen, Z. Li, Y. Liu, Surface chemical functional groups modification of porous carbon, Recent Patents on Chemical Engineering. 1 (1) (2008) 27-40.

[30] J. Zawadzki, Infrared-spectroscopy in surface-chemistry of carbons, Chem. Phys. Carbon. 21 (1989) 147-380.

[31] S. Tang, L. Sui, Z. Dai, Z. Zhu Z., H. Huangfu, High supercapacitive performance of Ni(OH)2/XC-72 composite prepared by microwave-assisted method. RSC Adv. 5 (2015) 43164-43171.

[32] M. A. Atieh, O. Y. Bakather, B. Al-Tawbini, A. A. Bukhari, F. A. Abuilaiwi, M. B. Fettouhi, Effect of Carboxylic Functional Group Functionalized on Carbon Nanotubes Surface on the Removal of Lead from Water, Bioinorg. Chem. Appl. 9 (2010) 1-10.

[33] J. A. Ardila, G. G. Oliveira, R. A Medeiros, O. Fatibello-Filho. Square-wave adsorptive stripping voltammetric determination of nanomolar levels of bezafibrate using a glassy carbon electrode modified with multi-walled carbon nanotubes within a dihexadecyl hydrogen phosphate film. Analyst, 139 (7) (2014) 1762-1768.

[34] F. C. Moraes, M. F. Cabral, L. H. Mascaro, S. A. S. Machado, The electrochemical effect of acid functionalization of carbon nanotubes to be used in sensors development, Surf. Sci. 605 (3) (2011) 435-440.

[35] Y. D. T. De Albuquerque, L. F. Ferreira, Amperometric biosensing of carbamate and organophosphate pesticides utilizing screen-printed tyrosinase-modified electrodes. Anal. Chim. Acta. 596(2) (2007) 210-221.

[36] L. Chen, B. Gu, G. Zhu, Y. Wu, S. Liu, C. Xu, Electron transfer properties and electrocatalytic behavior of tyrosinase on ZnO nanorod, J. Electroanal. Chem. 617 (1) (2008) 7-13.

[37] F. C. Vicentini, B. C. Janegitz, C. M. Brett, Fatibello-Filho, O. Tyrosinase biosensor based on a glassy carbon electrode modified with multi-walled carbon nanotubes and 1-butyl-3-methylimidazolium chloride within a dihexadecylphosphate film, Sens. Actuators, B. 188 (2013) 1101-1108.

[38] R. Han, L. Cui, S. Ai, H. Yin, X. Liu, Y. Qiu, Amperometric biosensor based on tyrosinase immobilized in hydrotalcite-like compounds film for the determination of polyphenols, J. Solid. State. Electrochem. 16 (2) (2012) 449-456.

[39] F. Kheiri, R. E. Sabzi, E. Jannatdoust, H. Sedghi, Acetone extracted propolis as a novel membrane and its application in phenol biosensors: the case of catechol, J. Solid. State. Electrochem. 15 (11-12) (2011) 2593-2599.

[40] Y. C. Tsai, C. C. Chiu, Amperometric biosensors based on multiwalled carbon nanotube-Nafion-tyrosinase nanobiocomposites for the determination of phenolic compounds, Sens. Actuators, B. 125 (1) (2007) 10-16.

[41] B. Wang, J. Zheng, Y. He, Q. Sheng, A sandwich-type phenolic biosensor based on tyrosinase embedding into single-wall carbon nanotubes and polyaniline nanocomposites, Sens. Actuators, B. 186 (2013) 417-422.

[42] B. Borisova, J. Ramos, P. Díez, A. Sánchez, C. Parrado, E. Araque, J. M. Pingarrón, A Layer-by-Layer Biosensing Architecture Based on Polyamidoamine Dendrimer and Carboxymethylcellulose-Modified Graphene Oxide. Electroanalysis, 27 (9) (2015) 2131-2138.

[43] J. M. Lee, G. R. Xu, B. K. Kim, H. N. Choi, W. Y. Lee, Amperometric Tyrosinase Biosensor Based on Carbon Nanotube-Doped Sol-Gel-Derived Zinc Oxide–Nafion Composite Films, Electroanalysis. 23 (4) (2011) 962-970.

[44] J. L. Smith, R. C. Krueger, Separation and purification of the phenolases of the common mushroom, J. Biol. Chem. 237(4) (1962) 1121-1128.

[45] S. Sotiropoulou, V. Vamvakaki, N. A. Chaniotakis, Stabilization of enzymes in nanoporous materials for biosensor applications. Biosens. Bioelectron. 20 (8) (2005)1674-1679.

[46] S. Kıralp, L. Toppare, Y. Yağcı, Immobilization of polyphenol oxidase in conducting copolymers and determination of phenolic compounds in wines with enzyme electrodes, Int. J. Bio. Macromol. 33 (1) (2003) 37-41.

Figure captions

Fig. 1. SEM images obtained for **(a)** CB and **(b)** CB-f nanoparticles in different magnifications: 40,000 × and 400,000 × (Inset).

Fig. 2. Nyquist plots obtained using the different electrodes (GCE, CB-DHP/GCE and CB-f-DHP/GCE) for 1.0×10^{-3} mol L^{-1} $K_3Fe(CN)_6$ in 0.1 mol L^{-1} KCl solution. All the spectra were recorded in the frequency range of 100 mHz to 100 kHz. Inset: **(a)** Comparison of Nyquist plots obtained for GCE and DHP/GCE. A remarkably increase at the R_{ct} is observed for the GCE surface modified only with DHP film. **(b)** Magnification of the high frequency region of Nyquist plots obtained for GCE, CB-DHP/GCE and CB-f-DHP/GCE, where the later electrode exhibited the lowest R_{ct}.

Fig. 3. CVs obtained in 0.075 mol L^{-1} phosphate buffer solution (pH 7.5) in the **(a, c)** absence and **(b, d)** presence of 1.0×10^{-4} mol L^{-1} catechol using **(a, b)** Tyr-CB-DHP/GCE and **(c, d)** Tyr-CB-f-DHP/GCE. Scan rate: 50 mVs^{-1}; Tyr concentration: 60 U.

Fig. 4. CVs obtained for 1.0×10^{-4} mol L^{-1} catechol in 0.075 mol L^{-1} phosphate buffer solution with pH ranging from 5.5 to 8.0 using the Tyr-CB-f-DHP/GCE biosensor. Scan rate: 100 mV s^{-1}. Inset: $-I_c$ *vs*. pH.

Fig. 5. Amperograms obtained for different catechol concentrations ((1) 1.0×10^{-6}, (2) 2.0×10^{-6}, (3) 4.0×10^{-6}, (4) 5.9×10^{-6}, (5) 7.9×10^{-6}, (6) 9.8×10^{-6}, (7) 1.9×10^{-5}, (8) 2.9×10^{-5} (8) and (9) 3.9×10^{-5} mol L^{-1}) in 0.075 mol L^{-1} phosphate buffer solution (pH 7.5) using the Tyr-CB-f-DHP/GCE biosensor. Applied potential = −0.2 V *vs.* Ag/AgCl. Inset: Analytical curve.

Fig. 6. Amperometric response of Tyr-CB-f-DHP/GCE biosensor towards the addition of different interfering substances in a 0.075 mol L^{-1} phosphate buffer (pH 7.5) solution containing

catechol a 5.0×10^{-6} mol L^{-1}. Applied potential = −0.2 V *vs.* Ag/AgCl; Interfering substances concentration = 5.0×10^{-5} mol L^{-1}.

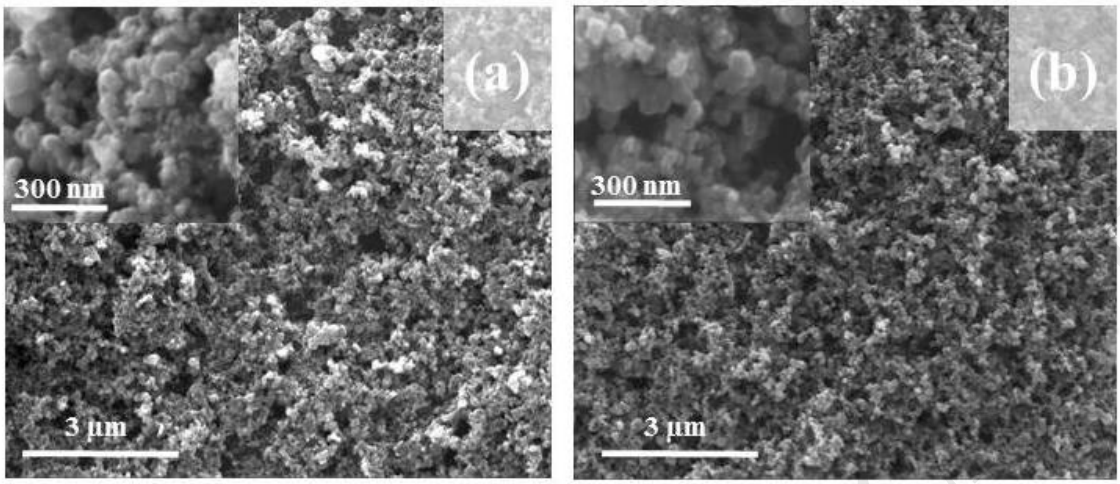

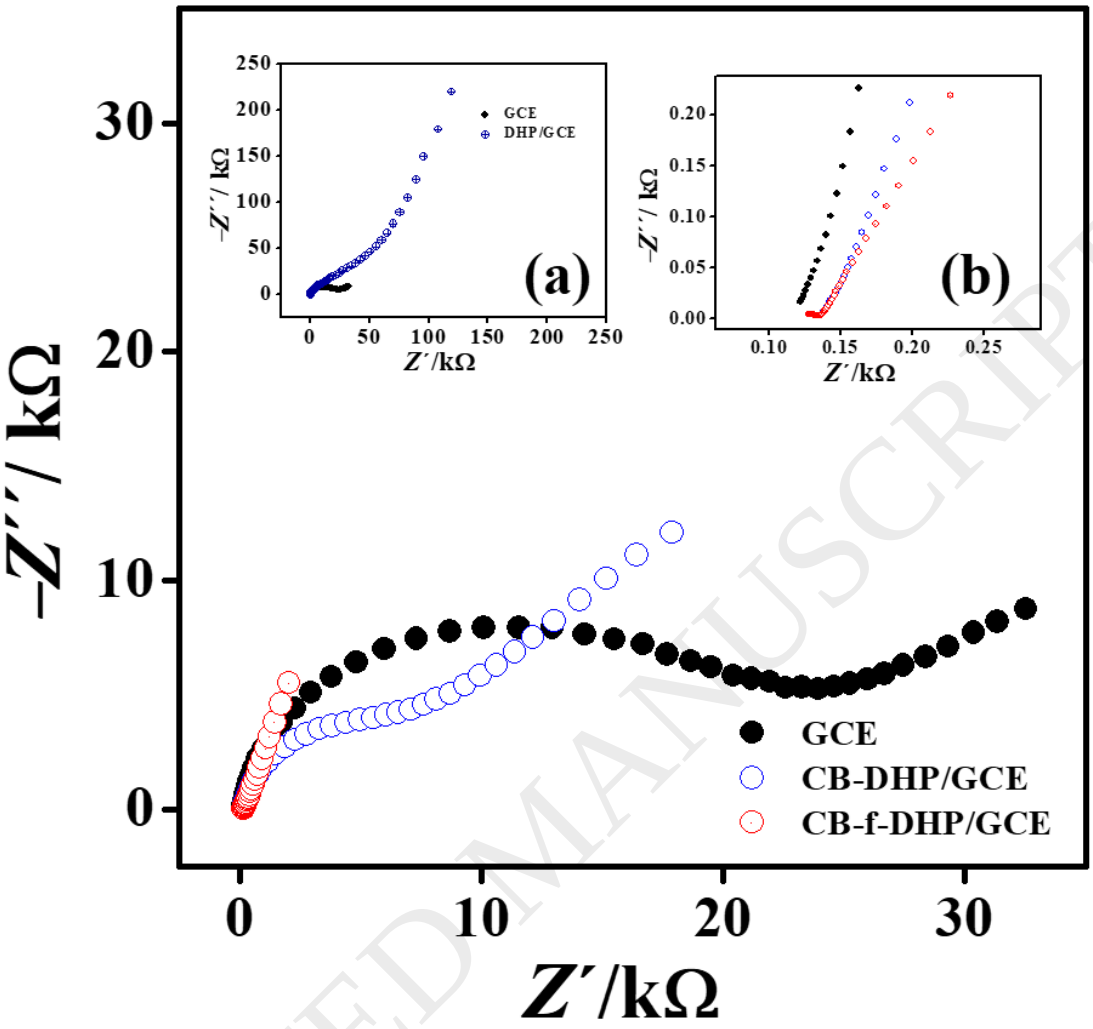

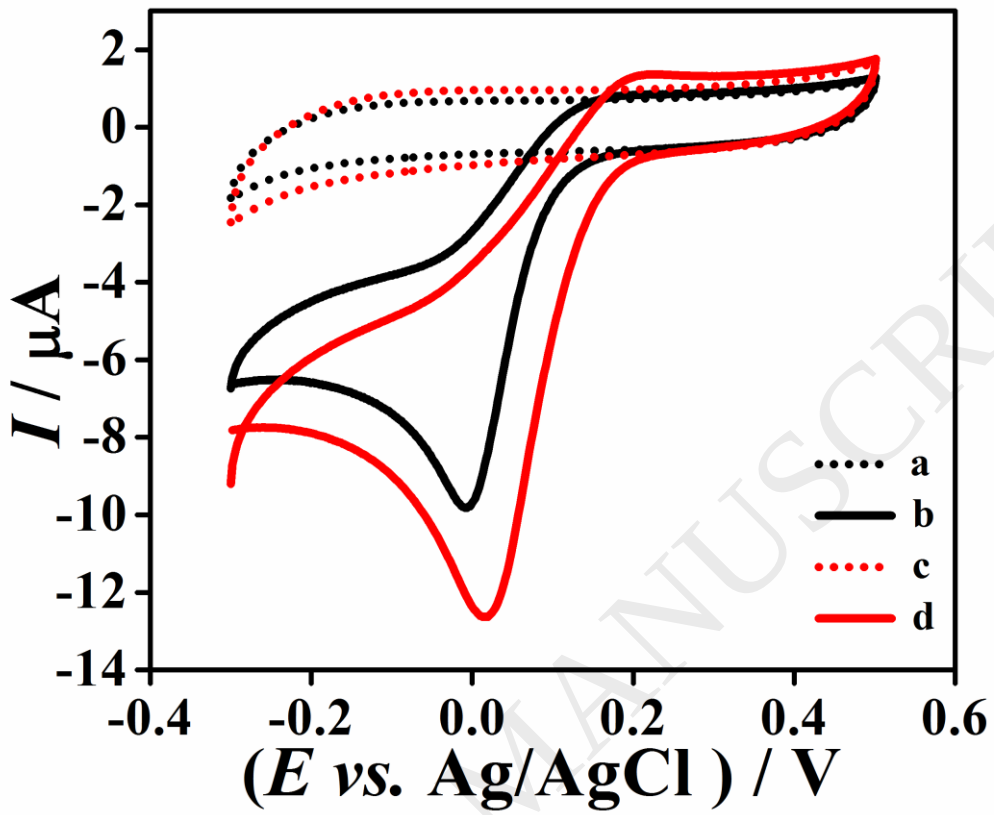

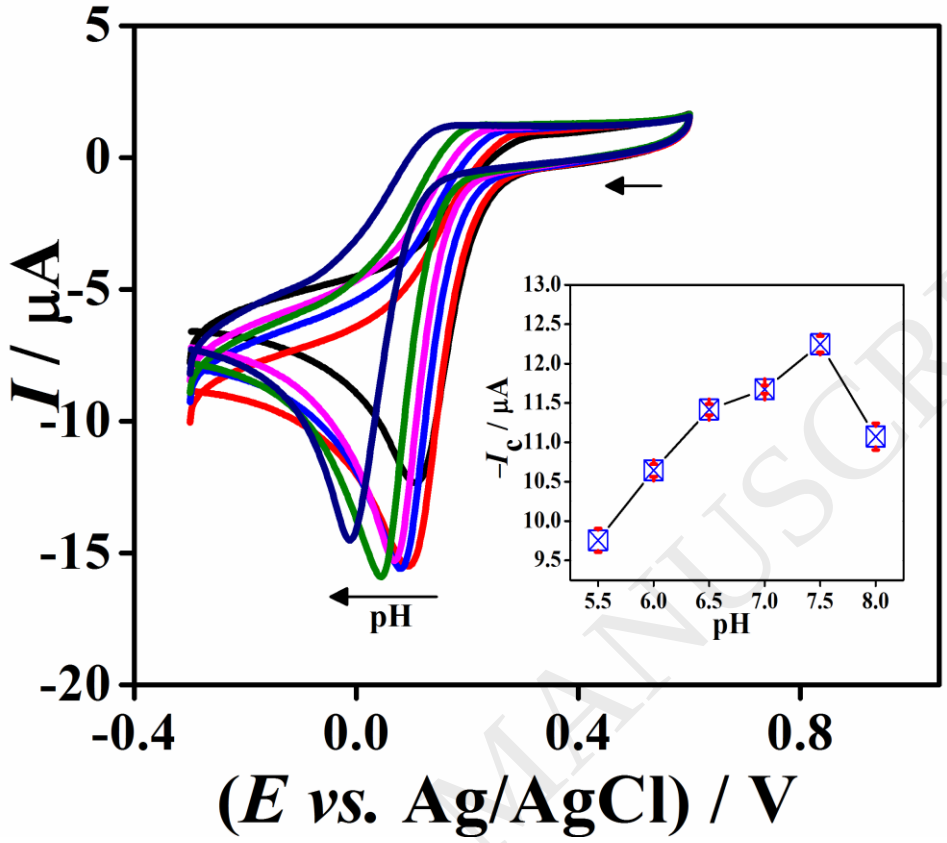

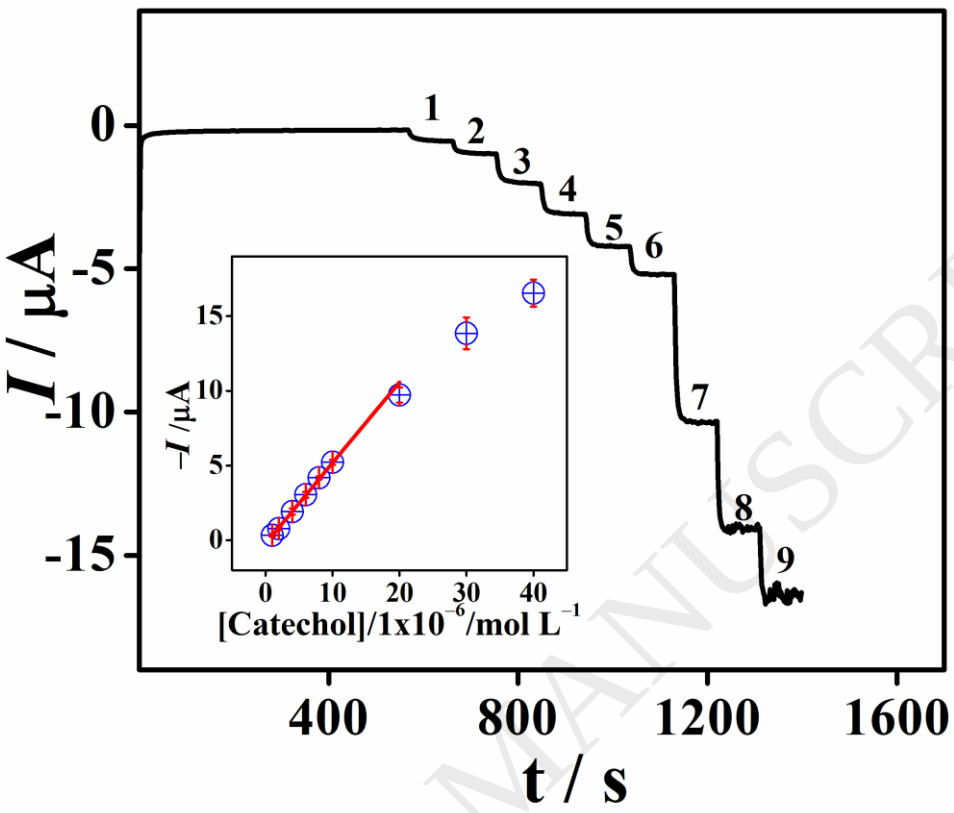

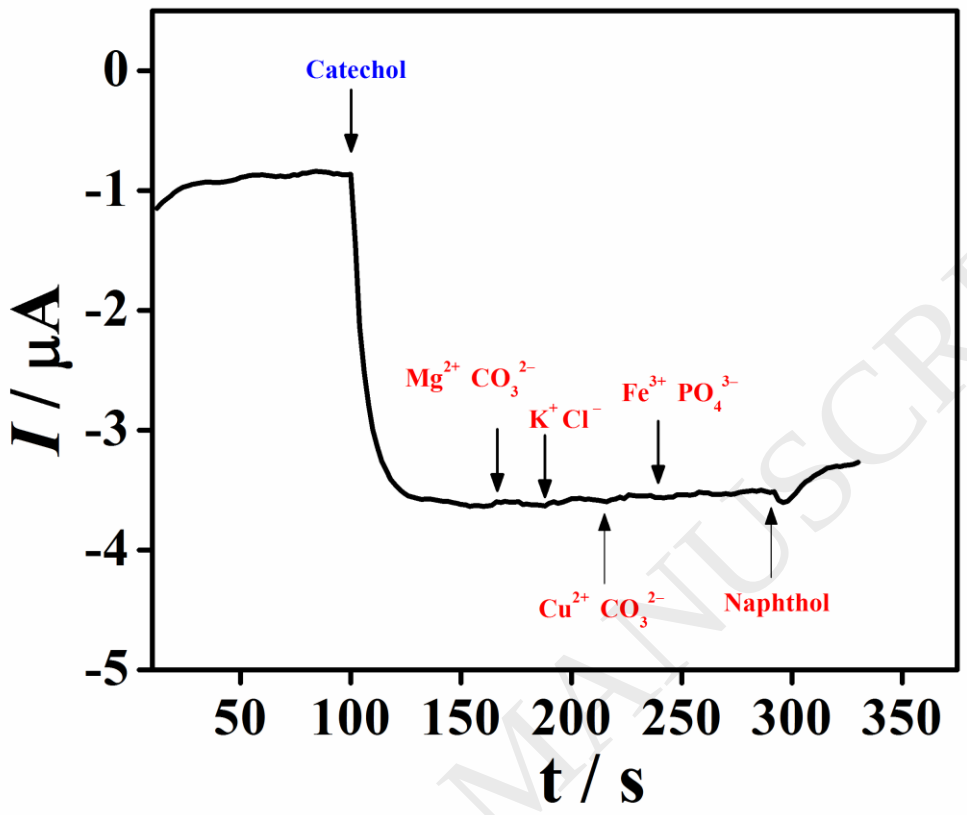

Tables

Table 1. Comparison of analytical parameters of Tyr biosensors for catechol determination.

Biosensor	Linear range (μmol L^{-1})	LOD (μmol L^{-1})	Sensitivity (mA mol^{-1} L)	Reference
Tyr-AuNPs-DHP/GCE	2.5–95	0.17	115	[26]
Nafion–Tyr–ZnO/GCE	10–1000	4.0	2.14	[36]
Tyr–IL–MWCNT–DHP/GCE	4.9–1100	0.58	32.8	[37]
Tyr/HTLc/GCE	3-300	0.1	----	[38]
Tyr/MWCNTs/AuNPs/AEP/Au	1.0 – 500	0.80	150	[39]
Tyr–Nafion–MWCNT/GCE	1–23	0.22	346	[40]
PANI/Tyr-SWCNTs	0.25-92	0.08	244	[41]
Tyr–PAMAN–GO–CMC/GCE	0.002–0.4	0.00090	630	[42]
Tyr–MWCNT–ZnO–Nafion/GCE	0.03–32	0.030	1890	[43]
Tyr–CB-f–DHP/GCE	**1–20**	**0.087**	**539**	**This work**

Table 2. Results of catechol recovery tests.

Sample	Catechol Concentration		Recovery / %
	Added / mol L^{-1}	Found / mol L^{-1}	
A	5.0×10^{-6}	$(4.7 \pm 0.4) \times 10^{-6}$	94
B	7.0×10^{-6}	$(6.9 \pm 0.5) \times 10^{-6}$	98
C	1.5×10^{-5}	$(1.48 \pm 0.08) \times 10^{-5}$	99